Physica Scripta. T90, 64–74, 2001

The Exterior and Interior Edge States of Magnetic Billiards: Spectral Statistics and Correlations

Klaus Hornberger[1,2] and Uzy Smilansky[2]

[1] Max-Planck-Institut für Physik komplexer Systeme, Nöthnitzer Straße 38, D-01187 Dresden, Germany
[2] The Weizmann Institute of Science, 76100 Rehovot, Israel

Received September 7, 2000

PACS Ref: 03.65.Ge, 05.45+b, 73.20.Dx

Abstract

We study the properties of quantum states in the interior and the exterior of magnetic billiards. A weight is associated to each state, providing an objective criterion to distinguish between bulk and edge states. We define a spectral density of edge states, which is then studied statistically and semiclassically. In particular, we observe strong cross-correlations between the interior and exterior edge spectra. They are identified as the quantum signature of a classical duality of periodic orbits.

1. Introduction

The boundary of a billiard partitions the plane into two distinct parts – the interior and the exterior. The dynamics in each part are quite different. The interior dynamics is always bounded. In the absence of a magnetic field, the exterior is a scattering problem, where the boundary serves as an obstacle. In spite of the different nature of the two systems, their intimate connection can be revealed by studying their corresponding Poincaré (bounce) maps. The two maps are related by a simple isomorphism, expressing the classical interior-exterior duality [1]. When quantized, the interior spectrum is pure point, while the exterior spectrum is continuous. The quantum interior-exterior duality enables the computation of the interior spectrum in terms of the exterior scattering matrix [2,3].

A homogenous magnetic field induces a velocity-dependent Lorentz force, which changes the classical dynamics considerably. For strong enough fields, the classical trajectories inside or outside either follow closed cyclotron orbits, or skip along the billiard boundary. Thus, the exterior dynamics is no longer unbounded. Like in the field free case, the Poincaré (bounce) maps for the exterior and the interior are isomorphic. (Strictly, this is true if the cyclotron radius is bounded away from the interval between the minimum and the maximum radii of curvature of the boundary).

The magnetic quantum spectra and wave functions reflect these classical properties. For strong fields, a separation takes place in the spectrum. Close to the Landau levels, one finds *bulk states* which correspond to the free cyclotron motion. In addition, *edge states* appear which are localised at the boundary, corresponding to the skipping motion. Unlike the field free case, the spectrum is purely discrete also in the exterior, with accumulation points at the energies of the Landau levels.

In the present work, we show that the quantum interior-exterior duality exists also for magnetic billiards, although it emerges in a different guise: It enforces a special correlation between the spectra of the interior and the exterior edge states.

The partition of the spectrum into "edge states" and "bulk states" seems intuitively clear, and it is often used [4–6]. However, the distinction between the two types is strict only in the extreme semiclassical limit. For finite $\hbar$ there exists a gradual transition between the two extremes, and we could not find in the literature any objective criterion to distinguish edge states from bulk states. Our first goal is, therefore, to propose an unambiguous spectral measure which accounts also for the existence of transitional states. This is done by attributing to each state a positive weight w_n which vanishes for extreme bulk states, and obtains a finite value for proper edge states. The precise definition of the ω_n will be given in Section 3. Equipped with the weights, the *edge state* density, in either the interior or the exterior, takes the form,

$$d_{\mathrm{edge}}(E) \;=\; \sum_{n=1}^{\infty} w_n \delta(E - E_n). \tag{1}$$

For the exterior, the sum extends formally over the infinite, near-degenerate spectral sets which accumulate at the Landau levels. However, due to an exponentially rapid decay of the weights for bulk states, they are in effect eradicated from $d_{\mathrm{edge}}(E)$.

The semiclassical form of the edge state density will be also discussed in Section 3. It provides the leading expressions for the smooth and the oscillatory parts of the spectral edge state density and suggests an interpretation of the weights in classical terms.

The definition of an edge state density (1) allows us to extend measures for spectral auto-correlations to the exterior problem. In Section 4.1 we compute the two-point form factors for the weighted quantum spectra, and show that they reproduce the predictions of random matrix theory (RMT), if they correspond to classically chaotic dynamics. The fact that this holds for the weighted exterior spectra suggests that the weights successfully focus on that component of the spectrum which is based on the phase space of classically chaotic bouncing orbits.

After that we are prepared to study the relation between the interior and exterior edge spectra. In Section 4.2 we show that there are strong, nontrivial cross-correlations on the quantum level. We argue that those are based on the generic existence of dual periodic orbits in the classical phase space of the interior and exterior problem.

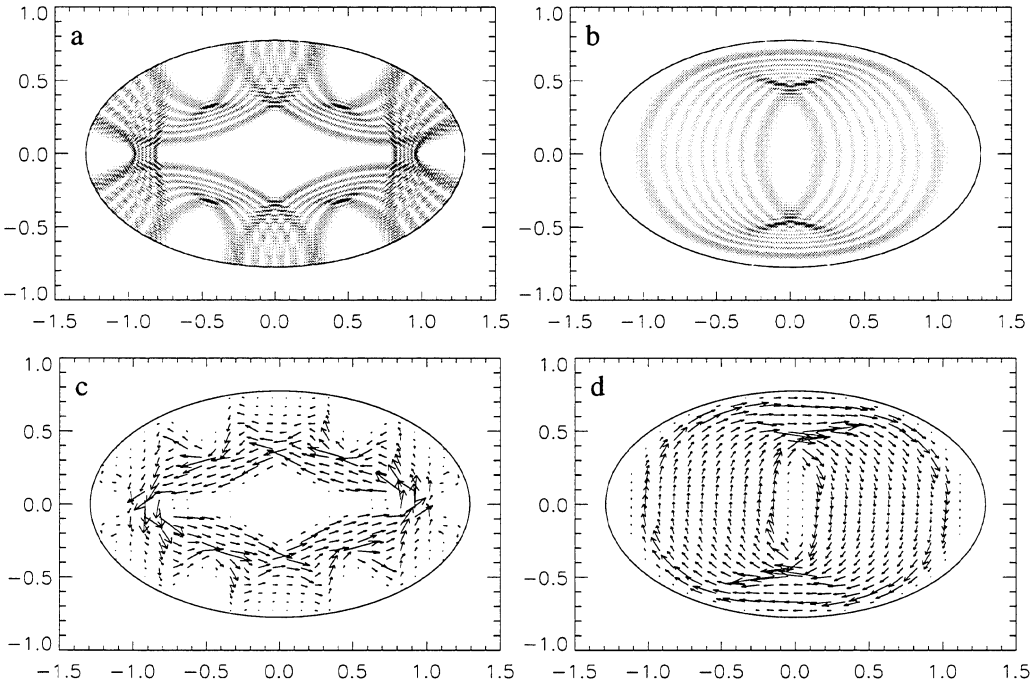

Fig. 1. Wave functions (a,b) and current distributions (c,d) in an elliptic domain at $\rho = 0.6$, around the ten-thousandth interior eigenstate, with energies $\nu \simeq 60.06026$ (a,c) and $\nu \simeq 60.50030$ (b,d).

2. The quantized magnetic billiard

To set the stage for the discussion of the edge state densities and their correlations, we give a brief overview of the magnetic Schrödinger problem for quantum billiards.

Consider a charged particle in $\mathbb{R}^2$, subject to a constant, perpendicular magnetic field of strength B. It is constrained to move either in the interior of a compact domain $\mathcal{D} \in \mathbb{R}^2$ or in the exterior $\mathbb{R}^2 \setminus \mathring{\mathcal{D}}$. The domain boundary $\Gamma = \partial\mathcal{D}$ is assumed to be smooth and its normals $\boldsymbol{n}(\boldsymbol{r})$ are defined to point outwards. The stationary Schrödinger equation reads

$$\frac{1}{2m}\left(-\mathrm{i}\hbar\nabla_r - q\boldsymbol{A}(\boldsymbol{r})\right)^2 \psi(\boldsymbol{r}) = E\,\psi(\boldsymbol{r}). \tag{2}$$

where m, q, and E denote the mass, charge, and energy of the particle, respectively. The vector potential in the symmetric gauge is $\boldsymbol{A} = (B/2)\,r\,\boldsymbol{e}_\vartheta$. Scaling time by the Larmor frequency $\omega = qB/(2m)$ reduces the parameters in (2) to the two length scales,

$$\rho^2 = \frac{E}{2m\omega^2} \qquad \text{and} \qquad b^2 = \frac{\hbar}{m\omega}, \tag{3}$$

Here, ρ is the cyclotron radius. Unlike this classical quantity, the magnetic length b has a pure quantum meaning. It gives the mean radius of a bulk ground state. The scaled energy may be expressed in terms of the spacing between Landau levels

$$\nu = \frac{E}{2\hbar\omega} = \frac{\rho^2}{b^2}. \tag{4}$$

The expression for the unscaled wave number $k = \sqrt{2mE}/\hbar = 2\rho/b^2$ indicates that there are two distinct short-wave limits: The high-energy limit $\rho \to \infty$ and the semiclassical limit $b \to 0$. The former corresponds to increasing the energy at fixed magnetic field while in the semiclassical limit one increases both energy and field, keeping ρ fixed. In this article we shall deal with "conventional" spectra (defined at fixed magnetic length b), unless explicitely stated otherwise (as in Section 4.1)

The Schrödinger equation is solved subject to the general gauge invariant boundary condition,

$$\psi = \pm\lambda\boldsymbol{n}(\boldsymbol{r})\left(\nabla_r\psi - \frac{\mathrm{i}}{b}\tilde{\boldsymbol{A}}(\boldsymbol{r})\psi\right), \quad \boldsymbol{r} \in \Gamma, \tag{5}$$

with $\tilde{\boldsymbol{A}} = 2/(Bb)\boldsymbol{A}(\boldsymbol{r})$ the scaled vector potential. The mixing parameter λ interpolates between Dirichlet ($\lambda = 0$) and Neumann ($\lambda^{-1} = 0$) boundary conditions. Equation (5) is a generalisation of the mixed boundary conditions known for the Helmholtz problem [7–9]. The lower sign in (5) corresponds to the exterior problem.

A very efficient technique to obtain precise spectra of quantum billiards is known as the boundary integral method. It allows to calculate ten-thousands of eigenvalues at a modest numerical effort. In a recent communication [10] we extended the method to the case of a finite magnetic field. For lack of space we cannot describe it here, and will make do with a few remarks. The boundary integral method reduces the Schrödinger equation (2) subject to the boundary condition (5) to an integral equation defined on the boundary. The (scaled) spectrum is given by the zeros of the corresponding Fredholm determinant. Also the wave functions can be calculated from the corresponding null vectors by a boundary integral.

The main problem of this approach at finite magnetic field is the occurrence of spurious solutions. In [10] we show that those can be related to physical solutions corresponding to a complementary problem at different boundary conditions. This allows us to construct an integral operator in terms of the regular free Green function which defines the spectrum uniquely. Employing special regularisation procedures to deal with the (hyper)-singular character of

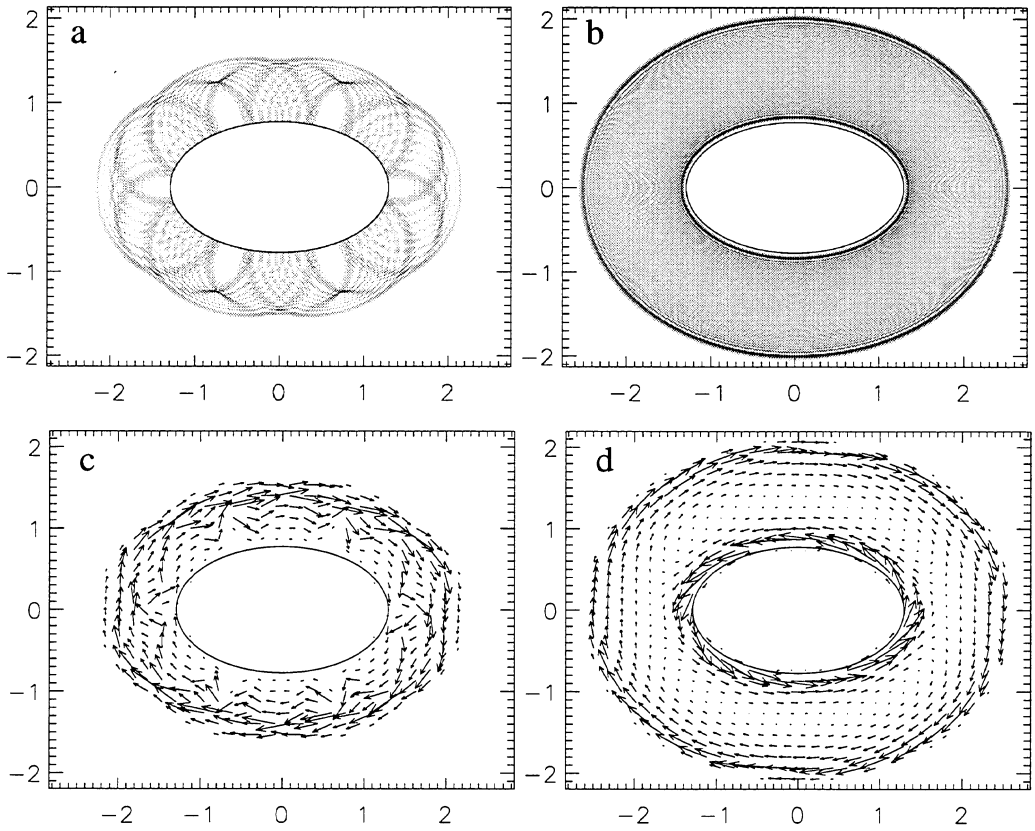

Fig. 2. Exterior wave functions (a,b) and current distributions (c,d) at $\rho = 0.6$ and at similar energies as in Fig. 1, $\nu \simeq 60.13634$ (a,c) and $\nu \simeq 60.50049$ (b,d).

the integral kernels, we obtain a stable and accurate numerical method. It allows to calculate the interior and the exterior spectra and wave functions for arbitrary boundary parameters λ.

An impression of interior and exterior edge and bulk states can be obtained from the wave functions shown in Figs. 1 and 2. We considered an elliptic domain with strong eccentricity ($\varepsilon = 0.8$, area $\mathcal{A} = \pi$) and energies corresponding to a cyclotron radius small enough to fit completely into the boundary.

Figure 1(a) shows the wave function of the approximately ten-thousandth interior eigenstate. In this semiclassical region of the spectrum, the wave functions tend to mimic the structures of the underlying classical phase space (which is mixed chaotic [11] in this case.) Clearly, Fig. 1(a) displays an edge state. Its probability density is localised along a stable interior periodic orbit bouncing 6×6 times along the boundary. Note, that the wave nature of this eigenstate is still visible at points where the trajectory crosses with itself, in particular at the shallow intersections close to the center. An interior bulk state – at a similar energy – is given in 1(b). Its wave function does not touch the boundary (i.e. the amplitude is exponentially small there.) Semiclassically, this state may be thought of as a superposition of closed cyclotron orbits. This can be seen clearly from the current distribution which is given in the bottom row of Fig. 1, where the length of the arrows is proportional to the amplitude of the current density.

Similar states can also be found in the exterior, as displayed in Fig. 2. The edge state, Fig. 2(a), belongs to an 8×6-orbit. Like all edge states it is distinguished from a typical bulk state, cf. Fig. 2(b), by the finite current it carries around the domain. In contrast, the bulk state with its counter-running current densities has no net current along the boundary, cf. Fig. 2(c) and Fig. 2(d).

In the next section, we shall develop an objective and quantitative criterion to resolve between bulk and edge states.

3. The spectral density edge of states

The intuition which led us to propose the definition of edge states can be best acquired by observing Fig. 3 which presents an *exterior* spectrum as a function of the boundary condition. Here, λ is parameterised by a value $\Lambda \in [-1; 0]$, $\lambda = \tan\big((\pi/2)\Lambda\big) \times b/(2\sqrt{\nu})$. We show the negative branch of λ because there the transition from Neumann ($\Lambda = -1$) to Dirichlet ($\Lambda = 0$) boundary conditions is continuous. (For positive λ this is not the case, a phenomenon known for the field free case [9], as well.)

The important observation to be made in this figure is that the states which accumulate near the Landau levels $\nu = N + \frac{1}{2}$, $N \in \mathbb{N}_0$ are extremely insensitive to the boundary condition employed. It is natural to associate these states with the bulk states – states which are only slightly affected by the existence of a boundary. In contrast, there are other states, whose energies depend strongly on the boundary condition. These are states which are naturally associated with the boundary – the edge states.

In the right part of Fig. 3 one can identify a sequence of bulk states which emanate from a Landau level and gradually turn into edge states. Clearly, it is the slope of the energy curves that provides a quantitative measure for the degree to which a state holds the character of an edge state. Moreover,

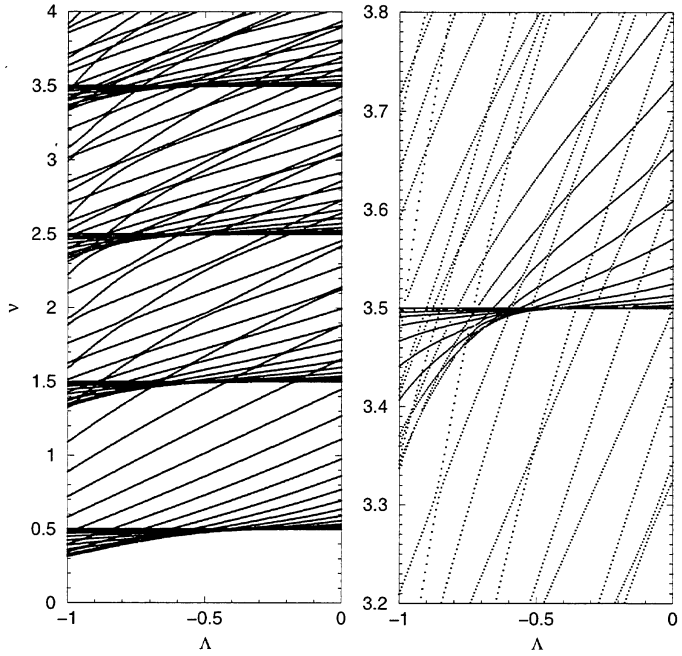

Fig. 3. The parametric dependence of the *exterior* spectrum on the boundary condition (for the asymmetric stadium [10] at fixed $b = 0.25$). The parameter Λ interpolates between Neumann ($\Lambda = -1$) and Dirichlet ($\Lambda = 0$) boundary conditions. The right graph shows details around the forth Landau level.

the asymptotic analysis reveals that these slopes decrease essentially like a Gaussian as one approaches the Landau level within a sequence of bulk states.

We therefore define the weights needed for the spectral density of edge states (1) as the derivatives of the energies ν_n with respect to the boundary mixing parameter at Dirichlet ($\lambda = 0$),

$$w_n := \frac{b}{2\sqrt{\nu}} \frac{\mathrm{d}\nu_n(\lambda)}{\mathrm{d}\lambda}\Big|_{\lambda=0}. \tag{6}$$

This way each Dirichlet state in the spectrum is weighted in terms of its sensitivity to a change of the boundary condition. Note, that this definition applies equally well for the interior and the exterior states. In the case of an exterior spectrum the infinite accumulation of bulk states is suppressed by the rapid decay of their weights. The prefactor in (6) was introduced in order to cancel the trivial energy dependence of the edge state weights and to render them dimensionless.

In Fig. 4 we show the weighted *exterior* spectrum of an elliptic billiard at constant $b = 0.1$. We plot the weights w_n of the exterior eigenstates against their energies ν_n. One clearly observes that the slopes serve to distinguish (bulk) states of vanishingly small w_n which accumulate at Landau levels $\nu = N + \frac{1}{2}, N \in \mathbb{N}_0$ from a finite set of states with appreciable w_n. Furthermore, the slopes account for the fact that there exists a number of intermediate states in the spectrum.

The formal way to define the spectral edge state density (1) is to consider the spectral counting function $N(\nu; \lambda)$,

$$N(\nu; \lambda) = \sum_{n=1}^{\infty} \Theta(\nu - \nu_n(\lambda)), \tag{7}$$

with Θ the Heaviside function. Taking the derivative with

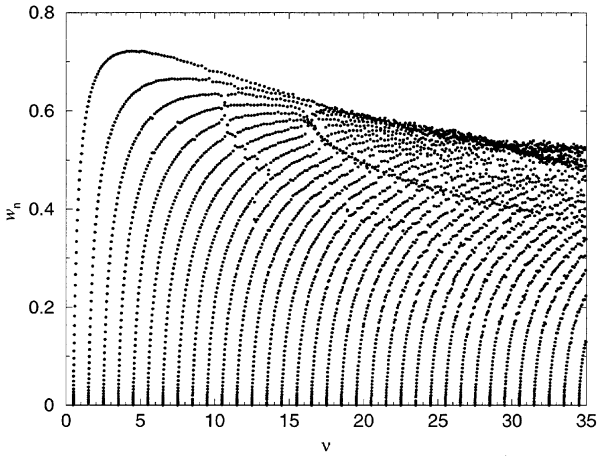

Fig. 4. Weighted spectrum of the *exterior* ellipse billiard (with eccentricity 0.8, area $= \pi$, magnetic length $b = 0.1$). Each point corresponds to a state with energy ν_n and weight w_n. There is an infinite number of bulk states at each Landau level $\nu = N + \frac{1}{2}$, characterised by vanishingly small weights.

respect to the boundary mixing parameter yields the spectral edge state density

$$d_{\mathrm{edge}}(\nu) := -\frac{b}{2\sqrt{\nu}} \frac{\partial N(\nu; \lambda)}{\partial \lambda}\Big|_{\lambda=0} = \sum_{n=1}^{\infty} w_n \, \delta(\nu - \nu_n). \tag{8}$$

Often, it is more convenient to deal with its integral, the edge state counting function

$$N_{\mathrm{edge}}(\nu) := \int_0^{\nu} d_{\mathrm{edge}}(\nu')\mathrm{d}\nu' = \sum_{n=1}^{\infty} w_n \, \Theta(\nu - \nu_n). \tag{9}$$

Again, the sum is formally over all states, including the bulk states. Since the contribution of the latter is eliminated by the rapid decay of the weights, its smooth part $\overline{N}_{\mathrm{edge}}(\nu)$ bears no marks of the Landau levels. One way to obtain the leading, curvature-independent term of $\overline{N}_{\mathrm{edge}}$ is to consider the magnetic disc billiard asymptotically (which is an integrable problem). The result is *identical* for the interior and exterior problem and proportional to the circumference $\mathcal{L}$ of the billiard, rather than its area:

$$\overline{N}_{\mathrm{edge}}(\nu) = \frac{2}{3} \frac{\mathcal{L}}{2\pi b} \nu^{3/2} + O(\nu). \tag{10}$$

It is proportional (by a factor 2) to the simple semiclassical estimate based on the classical phase space volume of skipping orbits.

Figure 5 shows the exterior edge state counting function (9) of the spectrum displayed in Fig. 4 after subtraction of the leading term (10). One observes that the infinite number of bulk states around each Landau level does not leave any marks in the edge counting function, apart from the first few Landau energies. This indicates that the proposed spectral measure succeeds to extract the important quasi one-dimensional states out of the spectrum. As one should demand its smooth part is to leading order proportional to the circumference rather than the area, and identical for interior and exterior problems.

The remaining oscillatory part of the edge state counting function

$$N_{\mathrm{edge}}^{\mathrm{osc}} = N_{\mathrm{edge}} - \overline{N}_{\mathrm{edge}}(\nu) \tag{11}$$

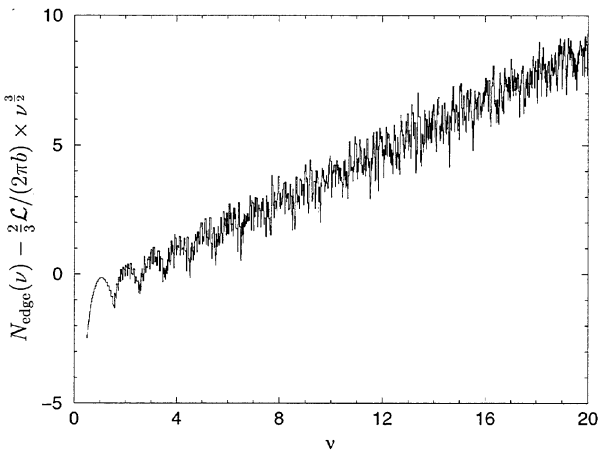

Fig. 5. Edge state counting function after subtraction of the leading part (10), calculated for the exterior spectrum shown in Fig. 4. The second order term is linear in ν and small compared to the leading order ($N_{\rm edge}(20) \approx 625$). The remaining, fluctuating part bears no marks of the Landau levels any more, apart from the first few.

can be described asymptotically as well, as discussed in the following.

3.1. *The periodic orbit sum for the edge state density*

The semiclassical trace formula for magnetic billiards can be derived by considering the semiclassical expressions for the integral operators of the boundary integral method. Using and extending the technique of Tasaki *et al.* [12] one can derive the explicit expression of the oscillatory parts of the spectral counting function $N(\nu;\lambda)$ for small but finite λ. This derivation is rather lengthy and will be reported in a forthcoming publication [13]. Unless otherwise specified, we shall consider hyperbolic systems, for which

$$N^{\rm osc}_{\rm skip}(\nu;\lambda) \approx \frac{1}{\pi}\sum_p \frac{1}{r_p D_p} \times \sin\left[S_p - \pi n_p - \frac{\pi}{2}\mu_p - 2\lambda\left(\frac{2\sqrt{\nu}}{b}\right)\sum_{i=1}^{n_p}\cos(\theta_i)\right]. \tag{12}$$

The sum is over all periodic orbits p which bounce n_p times at the boundary (with repetition number r_p). They have a reduced scaled action S_p (see below), μ_p conjugate points, and a stability matrix M_p which determines the stability denominator

$$D_p = |{\rm tr}(\mathsf{M}_p) - 2|^{\frac{1}{2}}. \tag{13}$$

Like in the non-magnetic case [9] the λ-dependence enters only as an additional phase, which depends on the angles of incidence θ_i with respect to the normal direction at the reflection points.

Taking the derivative with respect to the scaled boundary mixing parameter at Dirichlet, cf. equation (8), one obtains the semiclassical trace formula for the edge state density at Dirichlet boundary conditions,

$$d^{\rm osc}_{\rm edge}(\nu) = \frac{1}{\pi}\sum_p \frac{2\sum_{i=1}^{n_p}\cos(\theta_i)}{r_p D_p}\cos\left(2\pi\nu\sum_{i=1}^{n_p} t_i - \pi n_p - \frac{\pi}{2}\mu_p\right). \tag{14}$$

Here, we wrote the scaled action $S_p = 2\pi\nu\sum_i t_i$ in terms of the geometric contributions

$$t_i := \frac{1}{\pi}\left(\mathrm{asin}(\sigma_i) - \sigma_i\sqrt{1-\sigma_i^2} + \frac{\pi}{2} - \frac{\boldsymbol{r}_i \times \boldsymbol{r}_{i-1}}{2\rho^2}\right). \tag{15}$$

where

$$\sigma_i := \frac{\boldsymbol{r}_i - \boldsymbol{c}_{i-1}}{|\boldsymbol{r}_i - \boldsymbol{c}_{i-1}|} \times \frac{\boldsymbol{r}_i - \boldsymbol{r}_{i-1}}{|\boldsymbol{r}_i - \boldsymbol{r}_{i-1}|}. \tag{16}$$

characterises the arc between $\boldsymbol{r}_{i-1}$ and $\boldsymbol{r}_i$ around the center of motion $\boldsymbol{c}_{i-1}$

In contrast to (14), the unweighted density would be obtained by taking the derivative of (12) with respect to the energy ν. This yields the arclength $\partial S_p/\partial\nu = 2\sum_i(\pi/2 + \mathrm{asin}(\sigma_i))$ as a prefactor. (Note that ρ and σ_i are functions of ν). It shows that the periodic orbit sum for the edge state density differs from the unweighted one only by an additional prefactor

$$w_p = \frac{\sum_{i=1}^{n_p}\cos(\theta_i)}{\tau_p} \tag{17}$$

which attributes to each periodic orbit an individual classical weight. Since $\tau_p = \partial S_p/\partial(2\nu)$ is the (scaled) time of flight along the trajectory, we can interpret the weight (17) as the time averaged $\cos(\theta)$ for the periodic orbit.

In the limit of a "grazing" trajectory of many short arcs ($\sigma_i \to -1$), variations in the curvature of the boundary may be neglected and the classical weights w_p approach a value of unity. In the opposite case of an orbit which is almost detached from the boundary ($\sigma_i \to +1$), the weights vanish, since the cosines approach zero at a finite denominator. This justifies the omission of cyclotron orbits – which formally have zero weights – from the trace formula above. In contrast, the periodic orbit expression for the unweighted density of states would contain the contribution of cyclotron orbits (with a different order in $\hbar$) and would suffer divergencies at almost detached orbits [14].

It is instructive to compare the distributions of the quantum and classical weights. Unlike the quantum weights (6) attributed to each eigenvalue, the classical weights (17) are a property of the (periodic) orbits. In Fig. 6 we compare the phase space distribution of classical weights to the corresponding weighted quantum spectrum. The data was obtained for the interior elliptic billiard (cf. Fig. 1) and is given in both cases as a function of the classical cyclotron radius ρ. The distribution of classical weights $p(w_p)$ was approximated numerically by the histogram over a finite number of trajectories taken uniformly from phase space. Remarkably, one observes that the pronounced features of the distributions coincide. This finding is in some sense analogous to the known fact that wave functions tend to mimic classical phase space structures. It shows, that the quantum weights (which are defined originally in a quite formal way) do have a physical meaning, which translates to the classical dynamics.

Equipped with a well-defined spectral density and the corresponding trace formula, we can now proceed with a statistical and semiclassical study of edge state spectra. Here, we shall not only consider the statistics within an edge state spectrum, but also cross correlations between different, classically related spectra.

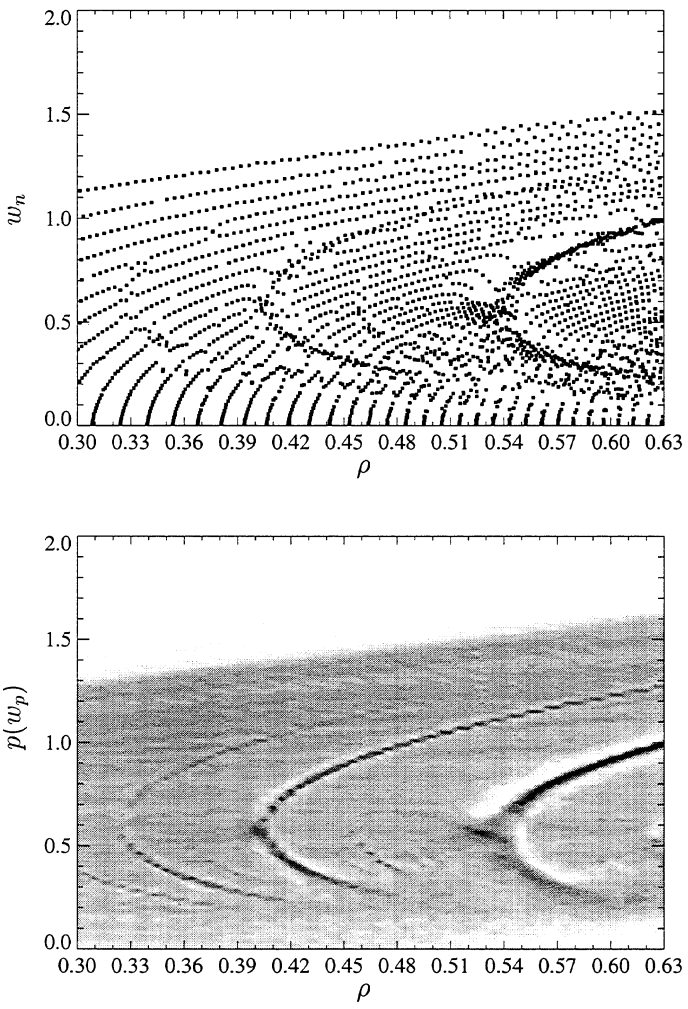

Fig. 6. Weighted quantum spectrum (top) and phase space distribution of the classical weights (bottom) for the interior ellipse. To facilitate comparison, also the quantum spectrum (calculated at constant $b = 0.1$, as in Fig. 4) is given in terms of the classical cyclotron radius ($\rho = b \times \sqrt{\nu}$.) One observes that the quantum weights tend to mimic the structures in the distribution of classical weights (which are due to stable islands in phase space.)

4. Spectral analysis

One of the central goals in the study of quantum chaos is to understand how the statistical properties of the quantum spectrum reflect the nature of the underlying classical dynamics. We extend this line of research to magnetic billiards, by making use of the weighted spectral measure discussed above. It was constructed to focus on the non-trivial part of phase space, which is determined by the billiard boundary map.

In the first part of this section we study the standard two-point auto-correlations – albeit for weighted spectral densities – in the interior and the exterior. They serve to identify generic spectral properties of hyperbolic systems (as described by random matrix theory.) The second part, in contrast, is concerned with a new kind of cross-correlation between the exterior and the interior spectra of complementary domains. It reveals the quantum finger-prints of the classical interior-exterior duality.

4.1. *Spectral auto-correlations*

A sensitive measure to characterise the spectral properties of a quantum system is provided by the form-factor $K(\tau)$, the (averaged) Fourier transform of the spectral 2-point autocorrelation function

$$R_{\nu_0}(\nu) = \int d^{\mathrm{osc}}_{\mathrm{edge}}\left(\nu' + \frac{\nu}{2}\right) d^{\mathrm{osc}}_{\mathrm{edge}}\left(\nu' - \frac{\nu}{2}\right) g_1(\nu' - \nu_0)\,\mathrm{d}\nu'. \tag{18}$$

Here, we included a normalized Gaussian window function g_1 to pick up a spectral interval centered at ν_0.

If the corresponding classical dynamics is hyperbolic the generic characteristics of a quantum spectrum should be reproduced by those of the appropriate ensembles of random matrix theory. However, before comparison to RMT it is necessary to remove the system dependent features of the spectrum by "unfolding" it. This is a transformation of the spectral density which renders it dimensionless and of unit density. Dealing with a *weighted* spectrum the unfolding procedure must transform both, the energies and the weights. The natural choice involves the smooth edge state counting function $\overline{N}_{\mathrm{edge}}$ and the mean weight $\langle w^2\rangle/\langle w\rangle$ in the spectral interval considered:

$$\tilde{\nu}_n = \frac{\langle w\rangle}{\langle w^2\rangle}\,\overline{N}_{\mathrm{edge}}(\nu_n) \tag{19}$$

$$\tilde{w}_n = \frac{\langle w\rangle}{\langle w^2\rangle}\,w_n. \tag{20}$$

Here, the first and second moments of the weights,

$$\langle w\rangle = \sum_{n=1}^{\infty} w_n\, g(\overline{N}_{\mathrm{edge}}(\nu_n) - \tilde{\nu}_0), \tag{21}$$

$$\langle w^2\rangle = \sum_{n=1}^{\infty} w_n^2\, g(\overline{N}_{\mathrm{edge}}(\nu_n) - \tilde{\nu}_0), \tag{22}$$

are taken locally in the spectrum in terms of the window function g (a normalised Gaussian of width σ.) As a result of this unfolding, both the weights and the weighted density, have unit mean.

Since we are dealing with a discrete spectrum, the form factor must be averaged. The standard procedure is to take the spectral average over non-overlapping parts of the spectrum,

$$K(\tau) = \left\langle \int \mathrm{e}^{2\pi\mathrm{i}\tilde{\nu}\tau} R_{\tilde{\nu}_0}(\tilde{\nu}) g_2(\tilde{\nu})\mathrm{d}\tilde{\nu} \right\rangle_{\tilde{\nu}_0}, \tag{23}$$

indicated by the triangular brackets. According to the spectral ergodicity hypothesis [15] this should be equivalent to an ensemble average.

The Wiener-Kinchin theorem holds in spite of the presence of window functions if we choose the widths of the Gaussians g_1 and g_2 as $\sigma/\sqrt{2}$ and $\sigma\sqrt{2}$, respectively. The form factor is then given by the *weighted* sum

$$K(\tau) = \left\langle \frac{2\sqrt{2\pi}\sigma}{\langle w^2\rangle} \left| \sum_{n=1}^{\infty} \tilde{w}_n \mathrm{e}^{2\pi\mathrm{i}(\tilde{\nu}_n - \tilde{\nu}_0)\tau} g(\tilde{\nu}_n - \tilde{\nu}_0) - \hat{g}(\tau) \right|^2 \right\rangle_{\tilde{\nu}_0}, \tag{24}$$

where the Fourier transform of g is denoted by $\hat{g}$.

Since we want to compare $K(\tau)$ to the prediction of random matrix theory, the corresponding classical dynamics should be hyperbolic throughout the whole spectrum considered. A convenient way to ensure this is to define the

spectrum in the semiclassical direction, i.e. at fixed cyclotron radius ρ, which renders the underlying classical phase space unchanged. The spectral variable v is increased in this case, by decreasing the magnetic length b. This can be done by increasing energy E and magnetic field B at fixed ratio E/B^2 and is equivalent to scaling down $\hbar$. The spectral edge density in the semiclassical direction is defined by taking the derivatives in (8) at fixed ρ. The smooth part of its counting function,

$$\overline{N}^{(\rho)}_{\mathrm{edge}}(v) = \frac{1}{2}\frac{\mathcal{L}}{2\pi\rho}v^2, \tag{25}$$

is again proportional to the circumference.

Using the numerical techniques described in [10] we calculated the interior and exterior weighted spectra at $\rho = 1.2$, for two different boundaries, the asymmetric stadium and the skittle billiard. These shapes (as defined in [10]) were chosen because they generate essentially hyperbolic classical motion at fairly strong magnetic fields. The asymmetric stadium has one reflection symmetry, while the skittle shape was constructed to have no symmetry. In combination with the magnetic field, the asymmetric stadium Hamiltonian therefore is invariant under an anti-unitary symmetry (reflection and time reversal) while the skittle is void of any symmetry.

For both shapes, complete cyclotron orbits with radius $\rho = 1.2$ do not fit into the interior domains. (Decreasing the cyclotron radius further would spoil hyperbolicity). As a consequence, one expects that all *interior* states are equal, concerning their edge state character. Indeed, the interior weights are distributed narrowly around a mean value $\overline{w}$ given by the ratio of weighted and unweighted mean densities $\overline{w} = \mathcal{L}\rho/(4\mathcal{A})$. The weights provide no additional information in this case, and one expects that the form factors are equal to those of the unweighted spectra, reproducing random matrix theory. In the upper row of Fig. 7 we show the interior form factors (24) of the asymmetric stadium and the skittle billiard. They indeed follow the RMT prediction of the Gaussian Orthogonal and Gaussian Unitary ensembles, respectively – as expected from the symmetry of their Hamiltonians. We note in passing, that it would have been more difficult to obtain the GUE form factor for a spectrum defined in the conventional high-energy direction, because with increasing energy the classical trajectories approach straight lines violating time-reversal invariance only minimally.

In contrast to the interior problem, the standard form factor does not exist for the unweighted exterior spectrum, which is dominated by infinitely many, bulk states. Only by considering a *weighted* spectrum did we obtain a well defined form factor. For the billiard shapes discussed above, also the exterior classical dynamics of the skipping orbits is (essentially) hyperbolic. As a crucial test for the appropriateness of the weights one should therfore demand that also the exterior form factor follows the standard RMT

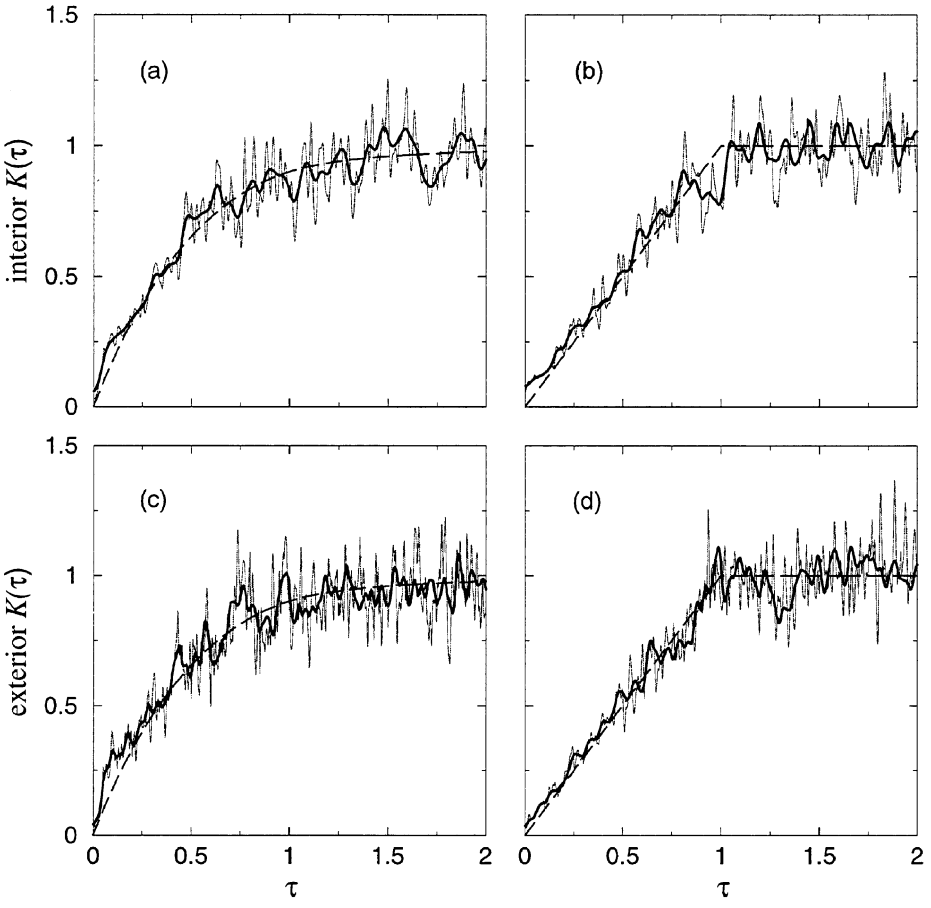

Fig. 7. Form factors of the weighted interior (a,b) and exterior (c,d) edge state spectra for the asymmetric stadium (a,c) and skittle (b,d) billiard, at $\rho = 1.2$. The functions follow the RMT predictions of the GOE and GUE ensembles, respectively (dashed lines). The heavy lines correspond to stronger spectral averaging than the thin lines ($\sigma_g = 10$ and $\sigma_g = 3$, resp.)

prediction. In the bottom row of Fig. 7 we display the form factors (24) calculated from the *exterior* edge state spectra of the two billiard shapes. One observes that they obey closely the predictions of random matrix theory. This proves that the weights as defined in (6) succeed to remove *selectively* the bulk state contributions out of the spectrum.

Most of the other popular measures characterising two-point spectral autocorrelations can be expressed in terms of the form factor and there is no need to discuss them any further.

4.2. *Spectral cross correlations*

From the quantum mechanical point of view it is hard to say, whether the interior edge spectrum should be related to the exterior one, and how this connection could possibly look like. Rather, it is classical dynamics that suggests that, indeed, there should be a strong, nontrivial correlation between the two quantum spectra.

The simple observation to be made is, that under rather general conditions the classical dynamics in the interior and exterior are *isomorphic*. This is the case, precisely, if any circle with the radius of a cyclotron orbit intersects the boundary at most twice. Then, due to simple geometry, every periodic orbit has a *dual* partner orbit, living in the complementary domain. They bounce along the boundary at the same points, complementing each other to full cyclotron circles. Each pair of orbits has the same stability and their actions sum up to an integer multiple of the action of a single cyclotron orbit.

Since it is the sets of periodic orbits that determine the spectra asymptotically, one should expect that the correlations in the bouncing orbits carry over to the edge spectra. In order to unravel the connection between interior and exterior edge state energies, a special cross-correlation function is needed. It not only involves the Dirichlet energies of the edge states but rests also on the information provided by their weights.

As the first step to obtain the appropriate correlator, we extend formally the definition of the edge state density to finite boundary mixing parameters λ. Using the scaled version $\Lambda = \lambda \times 2\sqrt{\nu}/b$ one can define

$$d_{\mathrm{edge}}(\nu;\Lambda) := -\frac{\partial}{\partial\Lambda} N_{\mathrm{skip}}\left(\nu;\frac{b}{2\sqrt{\nu}}\Lambda\right) \equiv -\frac{b}{2\sqrt{\nu}}\frac{\partial}{\partial\lambda} N_{\mathrm{skip}}(\nu;\lambda). \tag{26}$$

Below, the dependence of the spectral density on Λ will be needed only in the vicinity of the Dirichlet boundary condition $\Lambda = 0$. In this domain, the Λ-dependence may be expanded to first order. The weighted spectral density for small but finite Λ can then be written only in terms of the Dirichlet energies and Dirichlet weights:

$$\begin{aligned} d_{\mathrm{edge}}(\nu;\Lambda) &= \frac{b}{2\sqrt{\nu}}\sum_{n=1}^{\infty}\frac{\mathrm{d}\nu_n}{\mathrm{d}\lambda}(\lambda)\,\delta\big(\nu_n(\lambda)-\nu\big) \\ &\approx \frac{b}{2\sqrt{\nu}}\sum_{n=1}^{\infty}\frac{\mathrm{d}\nu_n}{\mathrm{d}\lambda}(0)\,\delta\Big(\nu_n(0)+\frac{2\sqrt{\nu}}{b}\frac{\mathrm{d}\nu_n}{\mathrm{d}\lambda}(0)\,\Lambda-\nu\Big) \\ &= \sum_{n=1}^{\infty}\delta\Big(\frac{\nu_n-\nu}{w_n}+\Lambda\Big). \end{aligned} \tag{27}$$

The cross-correlation function is now defined as an integral over energy and boundary parameter

$$C(\nu_0) = \iint d_{\mathrm{int}}^{\mathrm{osc}}(\nu;\Lambda)\, d_{\mathrm{ext}}^{\mathrm{osc}}(\nu;-\Lambda)\, h(\Lambda)\, g(\nu-\nu_0)\,\mathrm{d}\Lambda\,\mathrm{d}\nu \tag{28}$$

with normalized window functions h and g. Here, h serves to restrict the integration over Λ to the range where the linear approximation in (27) is valid and may have a width of order one. The function g, on the other hand, is necessary since we correlate discrete spectra. It selects a narrow energy interval centered around the energy ν_0 and should have the width of a few effective nearest neighbour spacings. Note, that unlike in Section 4.1, there is no averaging involved in the definition of the correlation function.

Substituting (27) in (28), the cross-correlation function assumes the form

$$C(\nu_0) = \sum_{i,j=1}^{\infty}\frac{w_i w_j'}{w_i+w_j'}\, g\left(\frac{\frac{\nu_i-\nu_0}{w_i}-\frac{\nu_0-\nu_j'}{w_j'}}{\frac{1}{w_i}+\frac{1}{w_j'}}\right) h\left(\frac{\nu_i-\nu_j'}{w_i+w_j'}\right) - C_{\mathrm{bg}}\ . \tag{29}$$

Here, the primes label the exterior energies and weights, for the sake of brevity. The important point to note in the double sum (29) is that due to the small width of g only a few pairs of interior and exterior spectral points will contribute appreciably at a given ν_0. It is the pairs with equal *weighted distances* from the left and right, respectively, to the reference energy ν_0. Here, the energy differences are scaled individually by the reciprocal weight attached to each spectral point. The function h, in contrast, limits the absolute energy distance. Note also, that the prefactor in (29) ensures that those pairs which include a bulk state do not contribute to the sum.

The term G_{bg} in (29) subtracts the background. It is approximated by

$$C_{\mathrm{bg}} \approx \overline{d}_{\mathrm{edge}}(\nu_0)\left(\sum_i h\left(\frac{\nu_i-\nu_0}{w_i}\right)+\sum_j h\left(\frac{\nu_j'-\nu_0}{w_j'}\right)-\overline{d}_{\mathrm{edge}}(\nu_0)\right), \tag{30}$$

if we neglect the width of g and disregard the fact that the higher order terms of the smooth edge densities differ for the interior and exterior.

We turn now to the semiclassical evaluation of the correlation function using the periodic orbit expressions discussed in Section 3. One obtains a double sum over the skipping interior and exterior periodic orbits

$$\begin{aligned} C(\nu_0) = \int \mathrm{d}\nu\, g(\nu-\nu_0)\ \frac{2}{\pi^2}\sum_{p,p'} w_p\frac{\tau_p}{r_p D_p}\, w_{p'}'\frac{\tau_{p'}'}{r_{p'}' D_{p'}'} \\ \times\Bigg\{\cos\Big(S_p+S_{p'}'-\pi(n_p+n_{p'}')-\frac{\pi}{2}(\mu_p+\mu_{p'}')\Big) \\ \times\hat{h}\left(\frac{1}{\pi}\sum_i\cos(\theta_i)-\frac{1}{\pi}\sum_j\cos(\theta_j')\right) \\ +\cos\Big(S_p-S_{p'}'-\pi(n_p-n_{p'}')-\frac{\pi}{2}(\mu_p-\mu_{p'}')\Big) \\ \times\hat{h}\left(\frac{1}{\pi}\sum_i\cos(\theta_i)+\frac{1}{\pi}\sum_j\cos(\theta_j')\right)\Bigg\}. \end{aligned} \tag{31}$$

Here, $\hat{h}$ is the Fourier transform of the window function h

and the exterior quantities are again marked with a prime. The width of $\hat{h}$ is small compared to the sum over $\cos(\theta_i)$ (which is of order n_p). As a result, the second term in the curly brackets of (31) is exponentially suppressed. Orbits with $\sum_i \cos(\theta_i) \approx 0$ that are not excluded by $\hat{h}$ are suppressed because of their vanishing classical weights as discussed at the end of Section 3.

In the first term of equation (31), $\hat{h}$ reduces the sum effectively to those pairs with approximately equal sums of angles of incidence $\sum_i \cos(\theta_i) = \sum_j \cos(\theta'_j)$. In most cases, only pairs of dual interior and exterior periodic orbits have this property. If p and p' are dual orbits their sum of actions is just a multiple of $2\pi v$ and also the other classical quantities are simply related:

$$\begin{aligned} n'_{p'} &= n_p, & r'_{p'} &= r_p, \\ S_p + S'_{p'} &= 2\pi v n_p, & \mu'_{p'} &= 2n_p - \mu_p, \\ D'_{p'} &= D_p, & w'_{p'}\,\tau'_{p'} &= w_p\,\tau_p. \end{aligned} \tag{32}$$

Keeping only the contributions of dual pairs of periodic orbits, the cross-correlation function assumes the form

$$C(v_0) = \frac{2}{\pi^2} \sum_p w_p^2 \left(\frac{\tau_p}{r_p D_p}\right)^2 \cos\bigl(2\pi n_p (v_0 - \tfrac{1}{2})\bigr)\ \hat{g}(n_p)\ . \tag{33}$$

Note, that retaining the contributions of dual pairs only, corresponds to the diagonal approximation used for the semiclassical evaluation of the *autocorrelation* function. However, here, the actions of the chosen pairs of periodic orbits complement each other, whereas in the standard diagonal approximation the resonant terms with $S_p - S_{p'} = 0$ give the dominant, "diagonal" contribution.

The energy dependence of the prefactor in (33) was neglected, since the variation of the energy was assumed to be small on the classical scale in (28). If v_0 is taken large (i.e. we are in the semiclassical regime of the spectrum) the classical quantities in (33) will hardly change as v_0 is varied. By grouping together the contributions from all the periodic orbits with the same number of reflections n_p, we obtain

$$C(v_0) = \sum_n f(n)\hat{g}(n) \cos(2\pi n(v_0 - \tfrac{1}{2})) \tag{34}$$

with

$$f(n) = \frac{2}{\pi^2} \sum_{p:n_p=n} w_p^2 \left(\frac{\tau_p}{r_p D_p}\right)^2. \tag{35}$$

Assuming ergodicity, the weighted sum over classical n-orbits (35) can be calculated as a phase space average. For large n it takes on the universal value $f(n) = n/8$. However, for a given cyclotron radius, the number of bounces n_p is bounded from bellow by $n_{\min} \approx \mathcal{L}/(2\rho)$. Hence $f(n < n_{\min}) = 0$.

Equation (34) makes a clear prediction on the form of the cross-correlation function. Even if the classical dynamics changes slowly as v_0 is varied, the infinite sum (34) will be appreciable only at energies $v_0 = N + \frac{1}{2}$, $N \in \mathbb{N}_0$, where the cosine terms are stationary. We expect the cross-correlation function therefore to display pronounced, equidistant peaks at large energies. These peaks are a direct manifestation of the existence of dual orbits. Their positions should coincide with the Landau levels.

This result should not be restricted to purely chaotic dynamics, although the bouncing map was assumed to be hyperbolic, so far. For integrable systems one obtains an analogous result. The semiclassical sum is then over rational tori rather than periodic orbits (with D_p describing their curvature.) The function $f(n)$ is not universal in this case, but the prediction remains that $C(v_0)$ is peaked at the energies of the Landau levels. The statement carries over to generic magnetic billiards, if we are allowed to approximate a mixed chaotic system by a union of non-overlapping hyperbolic and integrable phase space domains.

In Fig. 8 we display the cross-correlation function (29) for the ellipse billiard at magnetic length $b = 0.1$. It was calculated from the weighted spectra shown in Figs. 4 and 6. The corresponding classical dynamics is generic (mixed chaotic) and there is a strict, one-to-one correspondence between the interior and the exterior classical dynamics up to $v = 21.6$. Beyond this energy, when the cyclotron radius is greater than the minimum radius of curvature, the classical duality still holds in a substantial part of phase space.

One observes, that $C(v_0)$ is strongly fluctuating, but shows pronounced, equidistant peaks at energies $v_0 = N + \frac{1}{2}$. In Fig. 9 we focus on these dominant features by plotting the cross-correlation function in terms of $v_{\text{shift}} = v_0 (\text{mod } 1)$ around one half. To check that this clear signal is not a numerical artefact or due to the accumulation of bulk states, we make use of the fact that the spectra of the ellipse decompose into two symmetry classes. The cross correlation between exterior and interior spectra with *different* symmetries can be derived in a similar fashion as (34), however,

$$f(n) = \frac{2}{\pi^2} \sum_{p:n_p=n} (-1)^{\mu_p} w_p^2 \left(\frac{\tau_p}{r_p D_p}\right)^2. \tag{36}$$

where u_p counts the number of times the periodic orbit p crosses the symmetry line. Since u_p can be even or odd with equal probability for a given n, the expected cross-correlation should only show the background term. This is clearly supported by the numerical results shown as a dashed line in Fig. 9.

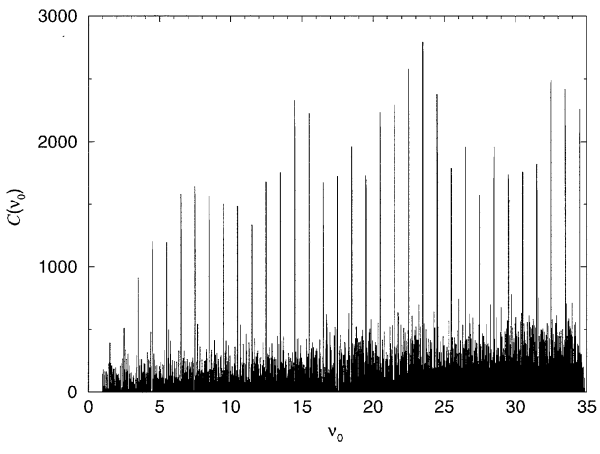

Fig. 8. Cross-correlation function (29) for the elliptic billiard ($\varepsilon = 0.8$, $b = 0.1$, $\sigma_g = 0.001$, $\sigma_h = 1$, positive part.) The pronounced peaks at $v_0 = N + \frac{1}{2}$, $N \in N_0$, indicate a nontrivial pair correlation between interior and exterior edge states.

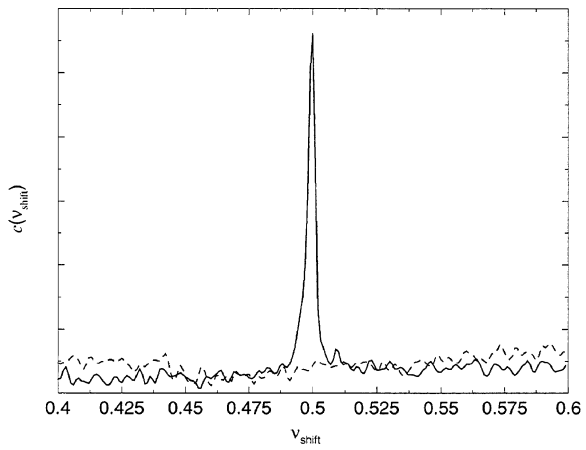

Fig. 9. Cross-correlation function of Fig. 8, summed over integer shifts of the argument, $c(\nu_{\text{shift}}) = \sum_n C(n + \nu_{\text{shift}})$. The energy pairs in (29) were taken within the same symmetry class (solid line) and between different symmetry classes (dotted line.)

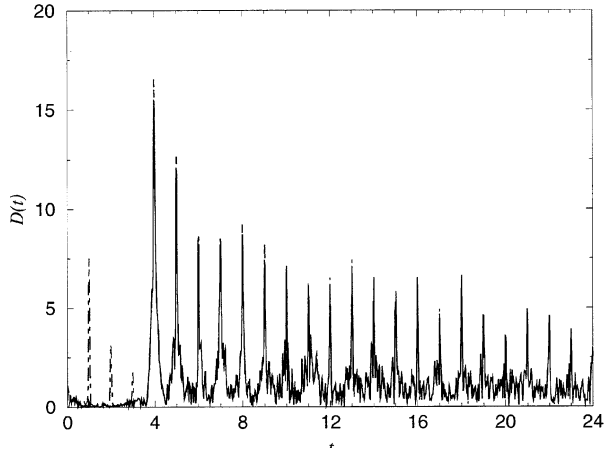

Fig. 10. Fourier transformation $D(t)$ of the cross-correlation function (absolute value). The peaks at integer t correspond to the combined actions of dual periodic orbits. If transitional states are disregarded (solid line compared to dashed line) the peaks vanish for $t < n_{\min} = 4$, but remain for $t \geq n_{\min}$.

The peaks in $C(\nu_0)$ were attributed semiclassically to the complementarity of classical actions of dual orbits. From the quantum point of view, their occurrence implies that there exists a nontrivial pairwise relation between individual interior and exterior edge states. This follows from the discussion of the quantum correlator (29) above. We have noted that pairs of edge energies contribute only if they have the same weighted distance to the reference energy from the left and right, respectively. Since $\nu_0 = N + \frac{1}{2}$, the interior energies ν_i and exterior energies ν'_j tend to appear in pairs, such that

$$\frac{\nu_i - (N - \frac{1}{2})}{w_i} \cong \frac{(N - \frac{1}{2}) - \nu'_j}{w'_j} \tag{37}$$

with integer N. This relation is not exact. It will be the more precise the larger and the closer the two energies are, since the semiclassical approximation (14) and the linearisation (27), respectively, will then hold the better. Nonetheless, in the spectra considered here, we could easily spot single pairs of edge states using relation (37) only.

Note, that the individual information provided by the quantum weights (or rather their ratio) plays a crucial role in this pair correlation. Other correlation functions, that involve only unweighted distances would not show any signal, in general. The way the quantum weights enter in (37) explains how a pairwise relation between interior and exterior states can exist in spite of different local densities. It is consistent with the fact that the mean edge densities are equal in the interior and exterior.

It should be mentioned that (37) can be inferred also without invoking periodic orbit theory, from the semiclassical relation between the unitary quantum operators of dual maps. We will discuss this issue in a later publication [13]. It is another indication that the peaks in the cross-correlation function are a generic semiclassical feature of dual magnetic billiards that is not restricted to hyperbolic systems.

As the last step, we consider the Fourier transform of the cross-correlation function, in order to analyse the fluctuating part of $C(\nu_0)$. The semiclassical prediction is a sequence of equidistant δ-spikes at integer values, starting from $n_{\min}$, the minimal number of reflections of the periodic orbits.

$$D(t) = \int C(\nu_0)\, \mathrm{e}^{-2\pi \mathrm{i} \nu_0 t} \mathrm{d}\nu_0 = \frac{1}{2} \sum_{n \geq n_{\min}} (-)^n f(n)\, \hat{g}(n)\, \delta(n - t). \tag{38}$$

We calculated the Fourier transform of the function $C(\nu_0)$ shown in Fig. 8. For these energies, the periodic orbits of the de-symmetrised ellipse have at least $n_{\min} = 4$ reflections.

Indeed, $|D(t)|$ displays distinct spikes at integer values (cf. Fig. 10, dashed line). One observes that the spikes are substantial starting from $t = 4$ (their real parts have signs $(-)^n$, as expected from the theory.) However, there are smaller peaks also at $t = 1, 2, 3$. To show convincingly that these are due to remnant contributions of transitional states, we calculated the cross-correlation function (29) disregarding all interior and exterior states with small weights (below 0.1 and 0.2, respectively). As a result, $C(\nu_0)$ is almost unchanged, and for $t \geq 4$ also its Fourier transform is very similar to the original one. However, the peaks below $t = 4$ now *vanish*, as can be seen from the solid line in Fig. 10. Therfore, if a more semiclassical part of the spectrum was considered – where a smaller fraction of the spectrum corresponds to transitional states – the remnant peaks would disappear. Nonetheless, the result proves that the cross-correlation function studied here succeeds to extract the relevant semiclassical information, and demonstrates unambiguously the quantum interior-exterior duality.

5. Conclusions

In this article, we proposed a conceptually clear and practicable spectral measure for edge states. The edge state density was found to suppress efficiently irrelevant bulk contributions – also for the exterior problem with its infinite number of bulk states. The weighted density facilitated the statistical analysis of interior and exterior spectra. We saw, that even in the exterior the spectral autocorrelations follow the predictions of random matrix theory, if the underlying

classical map is hyperbolic. Nontrivial cross-correlations between interior and exterior spectra were found to reflect the classical duality between the interior and the exterior classical bounce maps.

This duality is clearly stated for billiards for which a geodesic crosses the boundary at most twice. This is true for the magnetic and the field free billiards alike. However, in the field free case, one can define the interior and the exterior Birkhoff maps even for non-convex billiards, representing phase space by a manifold with several sheets. Here, the quantum duality holds for any shape. In the magnetic case, the classical problem was not yet studied in this respect, but the quantum correlations presented in Fig. 8 might indicate that the above condition is too restrictive.

Finally, the present work can be placed in a more general context than the spectral theory of edge states. The identification of a spectral cross correlation, which reveals an underlying classical duality appears in various possible applications and systems. Consider e.g., the Schrödinger operator on the surface of a sphere, subject to some standard boundary conditions on a closed curve. This is a billiard on the sphere, where the geodesics are large circles, and where the interior-exterior duality holds in complete analogy with the case of magnetic billiards. A more distant relative in this family of problems is the cross correlation of Dirichlet and Neumann spectra obtained for a single quantum billiard. The periodic orbits in the two systems are exactly the same, and the trace formulae differ only in the boundary phase by $(-1)^{n_p}$. Spectra which correspond to different representations of a symmetry groups fall in the same category.

Acknowledgements

We thank B. Gutkin and M. Sieber for helpful discussions. The work was partially supported by a Minerva fellowship for KH, and by the Minerva Center for Nonlinear Physics.

References

1. Doron, E. and Smilansky, U., Nonlinearity **5**, 1055 (1992).
2. Diez, B. and Smilansky, U., Chaos **3**, 581 (1993).
3. Eckmann, J.-P. and Pillet, C.-A., Commun. Math. Phys. **170**, 283 (1995).
4. Halperin, B. I., Phys. Rev. B **25**, 2185 (1982).
5. Gould, C. *et al.*, Phys. Rev. Lett. **77**, 5272 (1996).
6. Macris, N., Martin, P. A. and Pulé, J. V., J. Phys. A **33**, 1985 (1999).
7. Koshlyakov, N. S., Smirnov, M. M. and Gliner, E. B., "Differential Equations of Mathematical Physics", (North-Holland Publishing Company, Amsterdam, 1964).
8. Balian, R. and Bloch, C., Ann. Phys. (N.Y.) **60**, 401 (1970), erratum in Ann. Phys. **84** (1974), 559–563.
9. Sieber, M. *et al.*, J. Phys. A **28**, 5041 (1995).
10. Hornberger, K. and Smilansky, U., J. Phys. A **33**, 2829 (2000).
11. Robnik, M. and Berry, M. V., J. Phys. A **18**, 1361 (1985).
12. Tasaki, S., Harayama, T. and Shudo, A., Phys. Rev. E **56**, R13 (1997).
13. Hornberger, K. and Smilansky, U., in preparation.
14. Blaschke, J. and Brack, M., Phys. Rev. A **56**, 182 (1997), erratum in Phys. Rev. **A 57**, 3136 (1997).
15. Brody, T. A. *et al.*, Rev. Mod. Phys. **53**, 385 (1981).

